Supplemental Material

Contrasting roles of the RSC and ISW1/CHD1 chromatin remodelers in RNA polymerase II elongation and termination

Josefina Ocampo[1,2,*], Răzvan V. Chereji[1,*], Peter Eriksson[1], and David J. Clark[1,†]

[1]Division of Developmental Biology, *Eunice Kennedy Shriver* National Institute for Child Health and Human Development, National Institutes of Health, Bethesda, Maryland, USA
[2]Present address: Instituto de Investigaciones en Ingeniería Genética y Biología Molecular "Dr. Héctor N. Torres" (INGEBI-CONICET), Buenos Aires, Argentina
[*]These authors contributed equally to this work.
[†]Corresponding author. E-mail: clarkda@mail.nih.gov

Contents

Supplemental Methods

Estimation of average nucleosome spacing at the genome-wide level

To estimate the average nucleosome spacing at the genome-wide level, we aligned all yeast genes at their +1 nucleosomes, and computed the average nucleosome dyad density relative to the typical +1 nucleosome position. Then, we identified the positions of the peaks corresponding to the first five nucleosomes (+1, +2, +3, +4, +5) on the gene bodies, and we computed the average distance between these peaks using a simple linear regression (linear least squares fit). A custom graphical user interface (GUI) was developed in MATLAB, and is available on GitHub at:
`https://github.com/rchereji/Nucleosome_spacing_estimation/tree/GenomeRes_2019`

Estimation of average nucleosome spacing at the gene level

To estimate the average nucleosome spacing at the single gene level, the following the algorithm described in Ocampo et al. (2016), and reproduced below. We start with the nucleosome dyad profile, smoothed with a moving average filter with a span of 101 bp, y. For every gene, the window $[x_{+1} - 200, x_{+1} + 600]$ is selected, where x_{+1} represents the coordinate of the +1 nucleosome dyad. This window contains the NDR and the first four or five nucleosomes on the gene body. We construct a periodic pattern composed of six Gaussian distributions,

$$P_d(x) = G_0(x) + G_d(x) + G_{2d}(x) + G_{3d}(x) + G_{4d}(x) + G_{5d}(x),$$

where $G_D(x)$ represents a Gaussian distribution with mean D and standard deviation of 40 bp,

$$G_D(x) = e^{-\frac{(x-D)^2}{2\sigma^2}},$$
$$\sigma = 40.$$

We compute the cross-correlation between the smoothed dyad density $y([x_{+1} - 200, x_{+1} + 600])$ and the periodic pattern P_d([-200, 600]), with a lag s, $C(d, s)$, and we select the pair $\{d, s\}$ which maximizes the cross-correlation. Using this method, we obtain an estimation for the nucleosome spacing, d, and the shift of the nucleosome array, s, for every gene.

The custom MATLAB code for obtaining the gene-level estimation for the average nucleosome spacing in *Saccharomyces cerevisiae* is available on GitHub at:
`https://github.com/rchereji/Nucleosome_spacing_estimation/tree/GenomeRes_2019`

Supplemental Figures

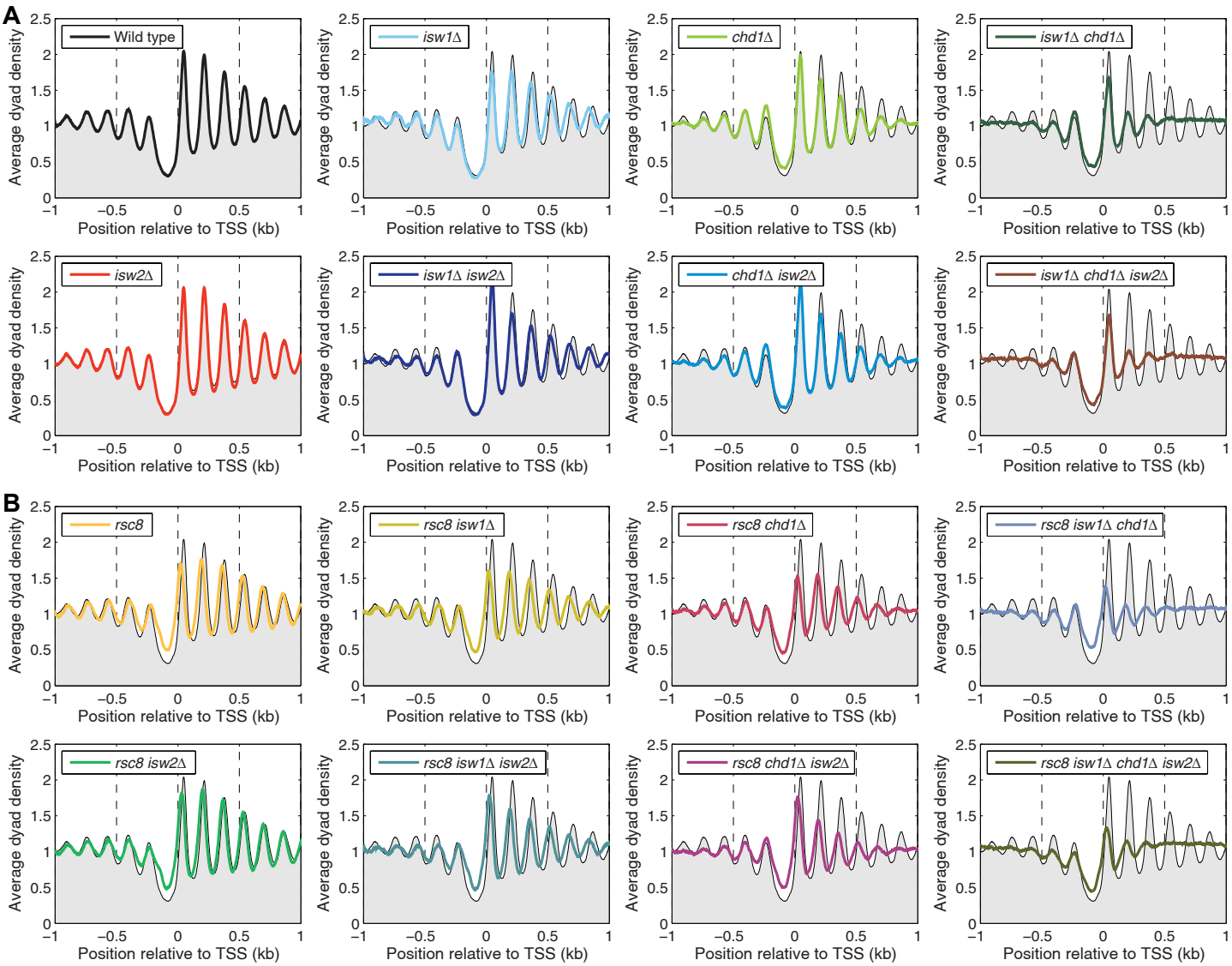

Supplemental Figure S1. Combinatorial effects of RSC, ISW1, CHD1 and ISW2 remodelers on the chromatin organization of yeast genes. Average nucleosome phasing on all yeast genes relative to the transcription start site (TSS) for all genes in wild type cells. (A) Phasing in wild type, *isw1*Δ, *chd1*Δ and *isw2*Δ mutants (Ocampo et al., 2016). (B) Phasing in *rsc8* mutants. For comparison, the phasing profile for wild type cells is shown in all plots (grey shading). The sequencing depths of all samples were normalized to 1 read per bp. See Fig. 1 for alignment on the +1 nucleosome.

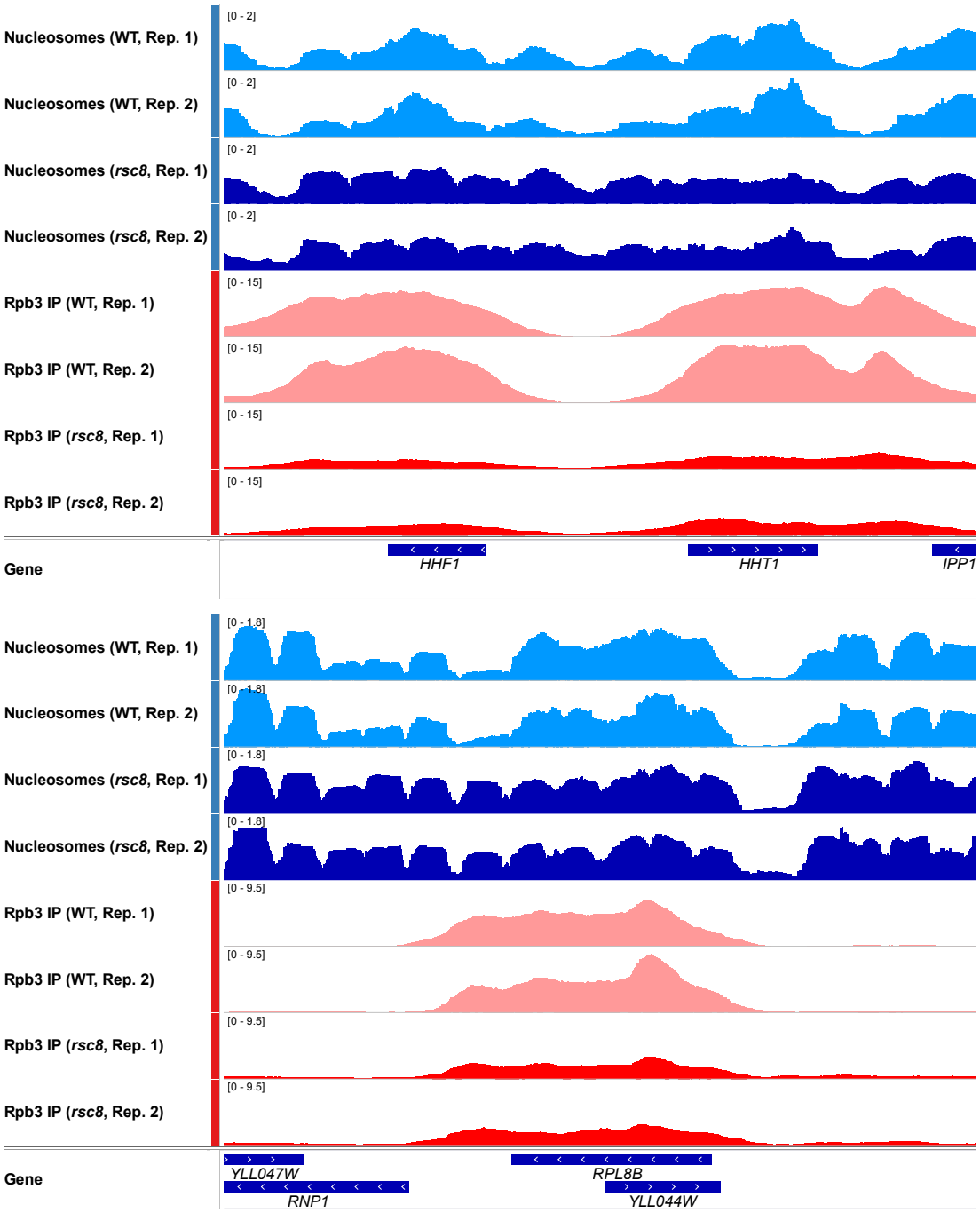

Supplemental Figure S2. IGV snapshots of *HHF1-HHT1* locus (A) and *RPL8B* gene (B). Downregulated genes (lower Rpb3 levels in the *rsc8* mutant) have more regular nucleosome arrays in the *rsc8* mutant, compared to wild-type cells. Blue tracks: nucleosome occupancy (MNase-seq data, 120-160 bp fragments); red tracks: Rpb3 occupancy (ChIP-seq data, 0-300 bp fragments).

A

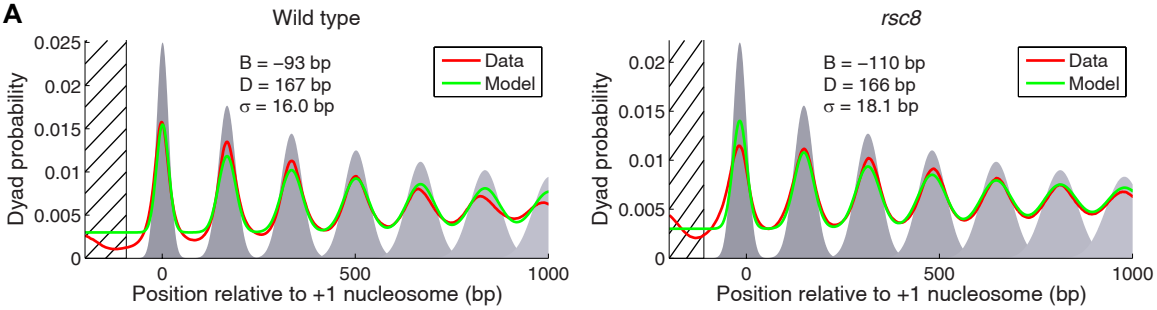

B

Strain	σ (bp)		**D** (bp)		**B** (bp)	
	Rep. 1	**Rep. 2**	**Rep. 1**	**Rep. 2**	**Rep. 1**	**Rep. 2**
Wild type	16.0	14.4	167	166	-93	-92
rsc8	18.1	18.5	166	166	-110	-109
*isw1*Δ	18.9	18.4	160	159	-87	-84
*chd1*Δ	20.2	19.5	167	165	-96	-91
*isw2*Δ	15.3	16.1	166	168	-90	-95
*rsc8 isw1*Δ	21.3	21.7	162	162	-107	-105
*rsc8 chd1*Δ	23.9	25.1	162	164	-107	-110
*rsc8 isw2*Δ	19.3	20.4	167	167	-106	-101
*isw1*Δ *chd1*Δ	27.5	28.1	160	160	-88	-87
*isw1*Δ *isw2*Δ	18.9	21.3	161	165	-87	-93
*chd1*Δ *isw2*Δ	20.0	20.5	168	165	-96	-90
*rsc8 isw1*Δ *chd1*Δ	31.1	31.1	153	154	-96	-98
*rsc8 isw1*Δ *isw2*Δ	22.3	22.9	162	161	-103	-98
*rsc8 chd1*Δ *isw2*Δ	26.0	25.1	167	163	-110	-105
*isw1*Δ *chd1*Δ *isw2*Δ	30.2	28.8	160	159	-84	-85
*rsc8 isw1*Δ *chd1*Δ *isw2*Δ	33.0	35.6	155	155	-91	-86

Supplemental Figure S3. Phasing parameters for chromatin remodeler mutants. The active nucleosome positioning model (Ganguli et al., 2014) was used to estimate the typical position of a nucleosome relative to its neighbors: D - average distance; σ - standard deviation (characterizing the degree of nucleosome phasing); B - position of the barrier edge relative to the typical location of +1 nucleosome dyad in wild type cells. (A) Examples of the fitted nucleosome distribution (red line - data; green line - model) for wild type cells (left) and *rsc8* cells (right). (B) Summary of the fitted parameters for all yeast strains used in this study. See (Ganguli et al., 2014) for a full description of the model.

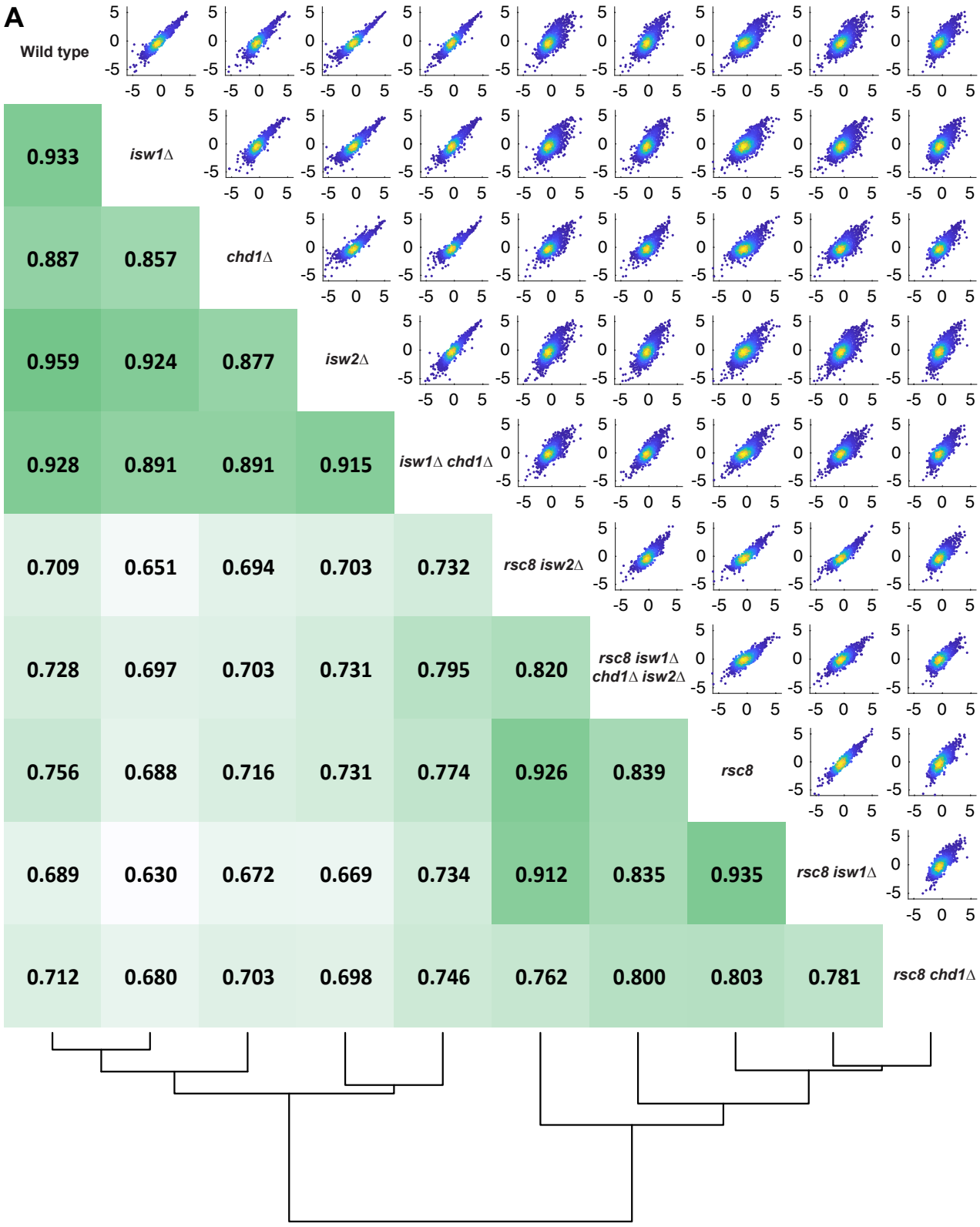

Supplemental Figure S4. Hierarchical clustering of wild type cells and remodeling mutants using the correlation between average RNA polymerase II distribution on all yeast genes. (A) Above the main diagonal: density scatter plot of $\log_2$(Avg. Pol II density) for different strains, indicated on the diagonal. Below the main diagonal: Spearman's rank correlation coefficients between the transcription levels in the corresponding strains. Bottom: hierarchical clustering dendrogram showing the formation of two clusters: one containing the *rsc8* mutants and one containing the other cell types. The dendrogram was produced in R using the `pheatmap` function (complete linkage method). The correlation coefficients between the 2 replicates of each experiment are: 0.976 (WT), 0.955 (*isw*1Δ), 0.967 (*isw*2Δ), 0.887 (*chd*1Δ), 0.973 (*rsc*8), 0.982 (*isw*1Δ *chd*1Δ), 0.967 (*rsc*8 *isw*1Δ), 0.957 (*rsc*8 *isw*2Δ), 0.925 (*rsc*8 *chd*1Δ), 0.791 (*rsc*8 *isw*1Δ *chd*1Δ *isw*2Δ).

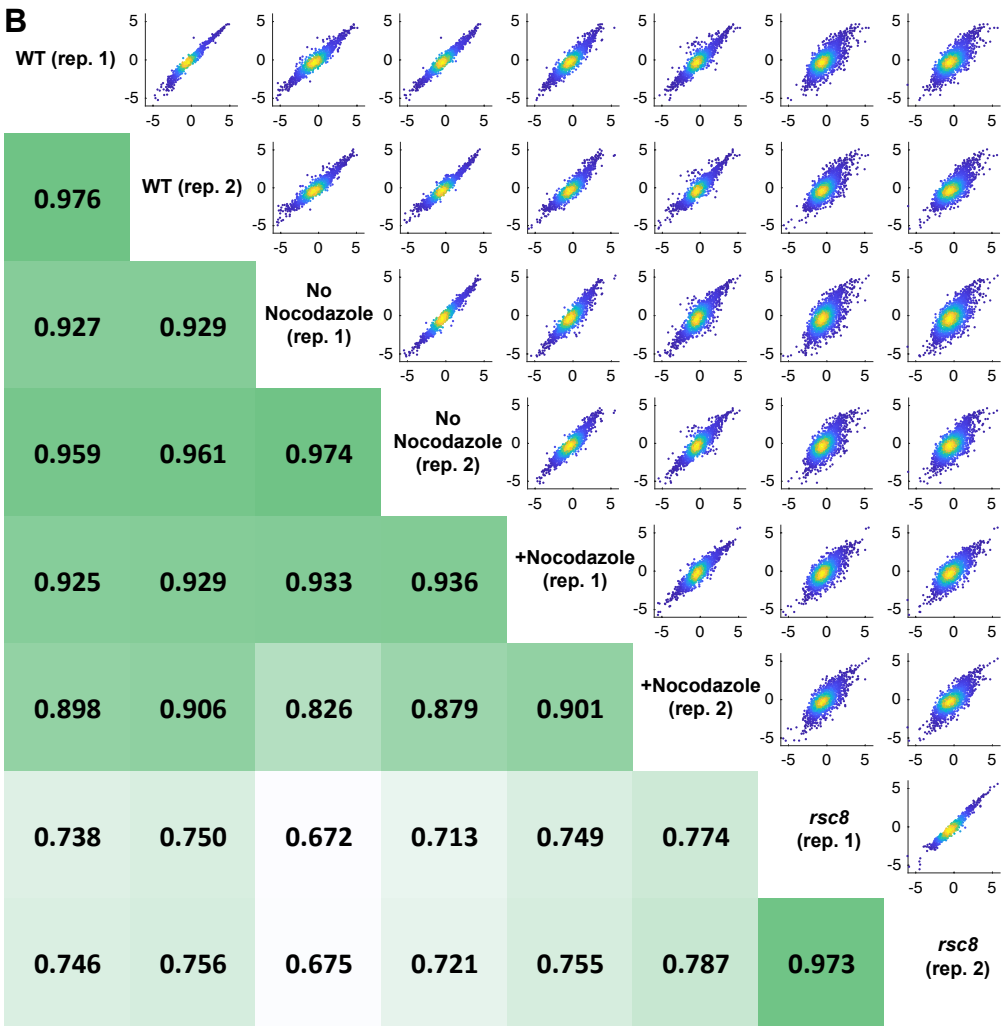

Supplemental Figure S4. (Continued.) (B) Density scatter plot showing the effect of 2h of Nocodazole treatment on gene expression.

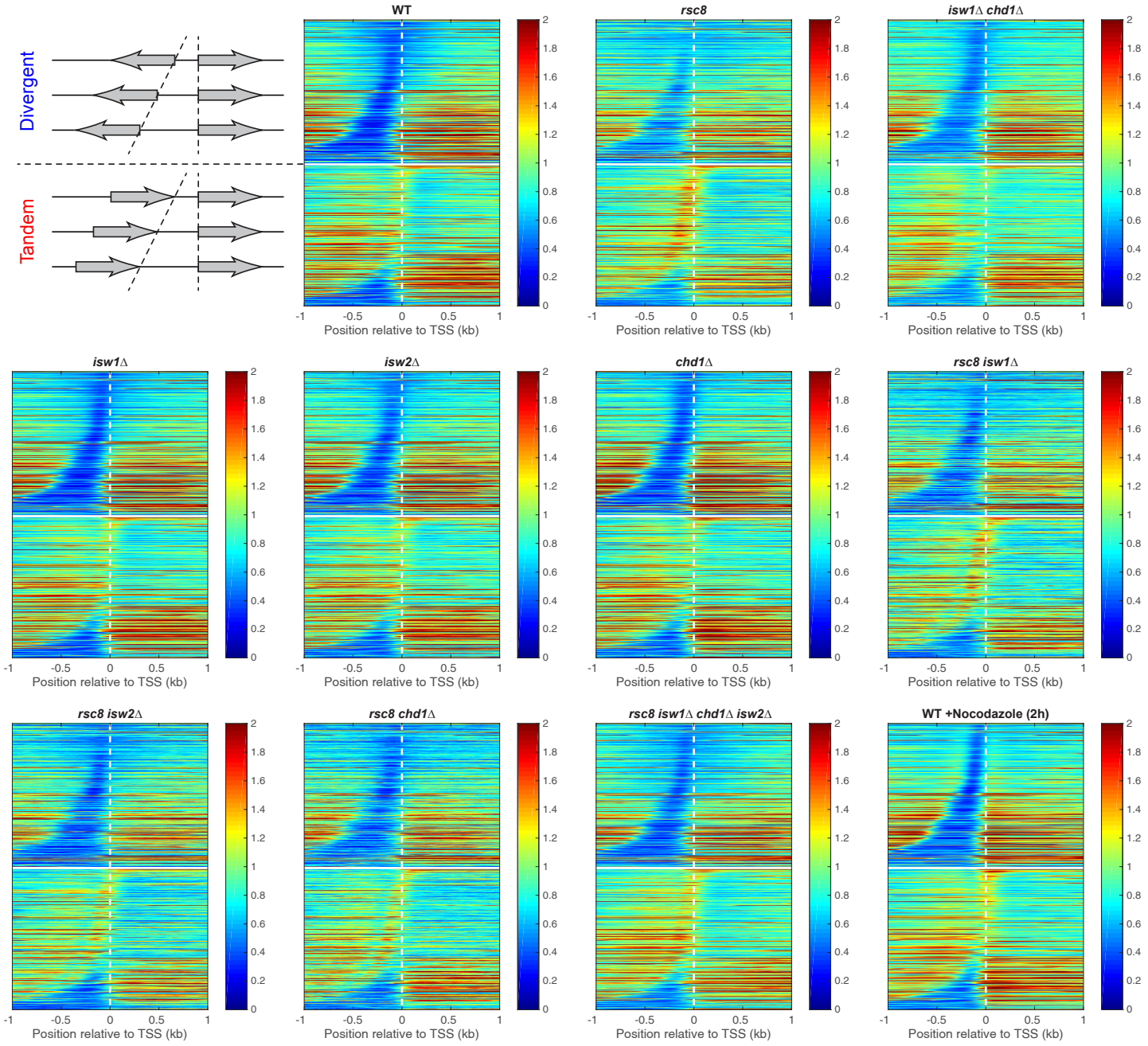

Supplemental Figure S5. Heat maps for the Rpb3 distribution for all strains. Genes were aligned and sorted as in Fig. 3A. The white horizontal line separates divergent (top) from tandem gene pairs (bottom).

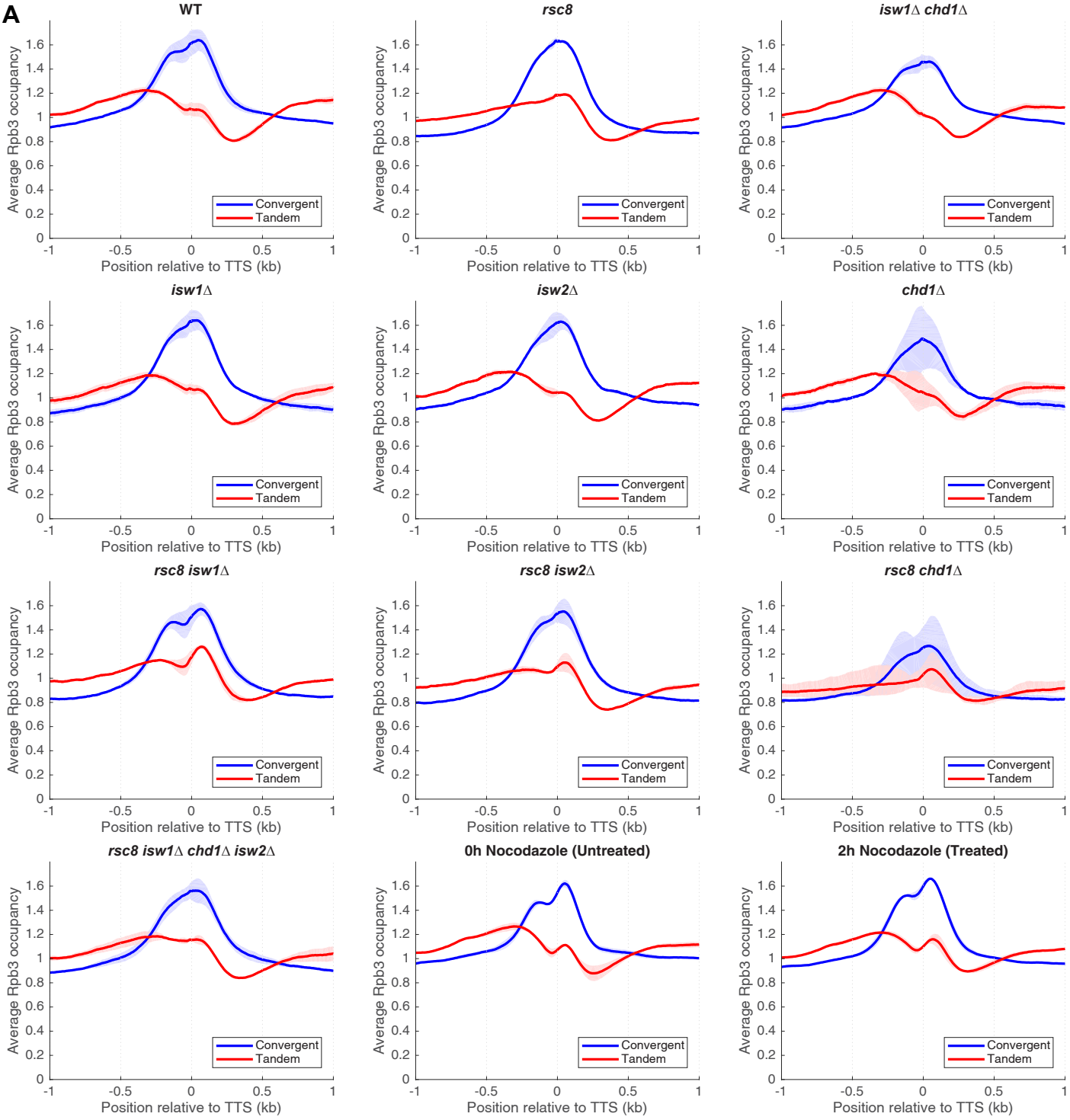

Supplemental Figure S6. RSC and ISW1/CHD1 have opposite effects on the levels of elongating and terminating Pol II: Alignment on the transcript termination site (TTS). Data for all strains. (A) Aggregate plots for Pol II occupancy relative to the TTS of the upstream gene for convergent and tandem gene pairs. ChIP-seq fragment sizes used: $\leq$300 bp.

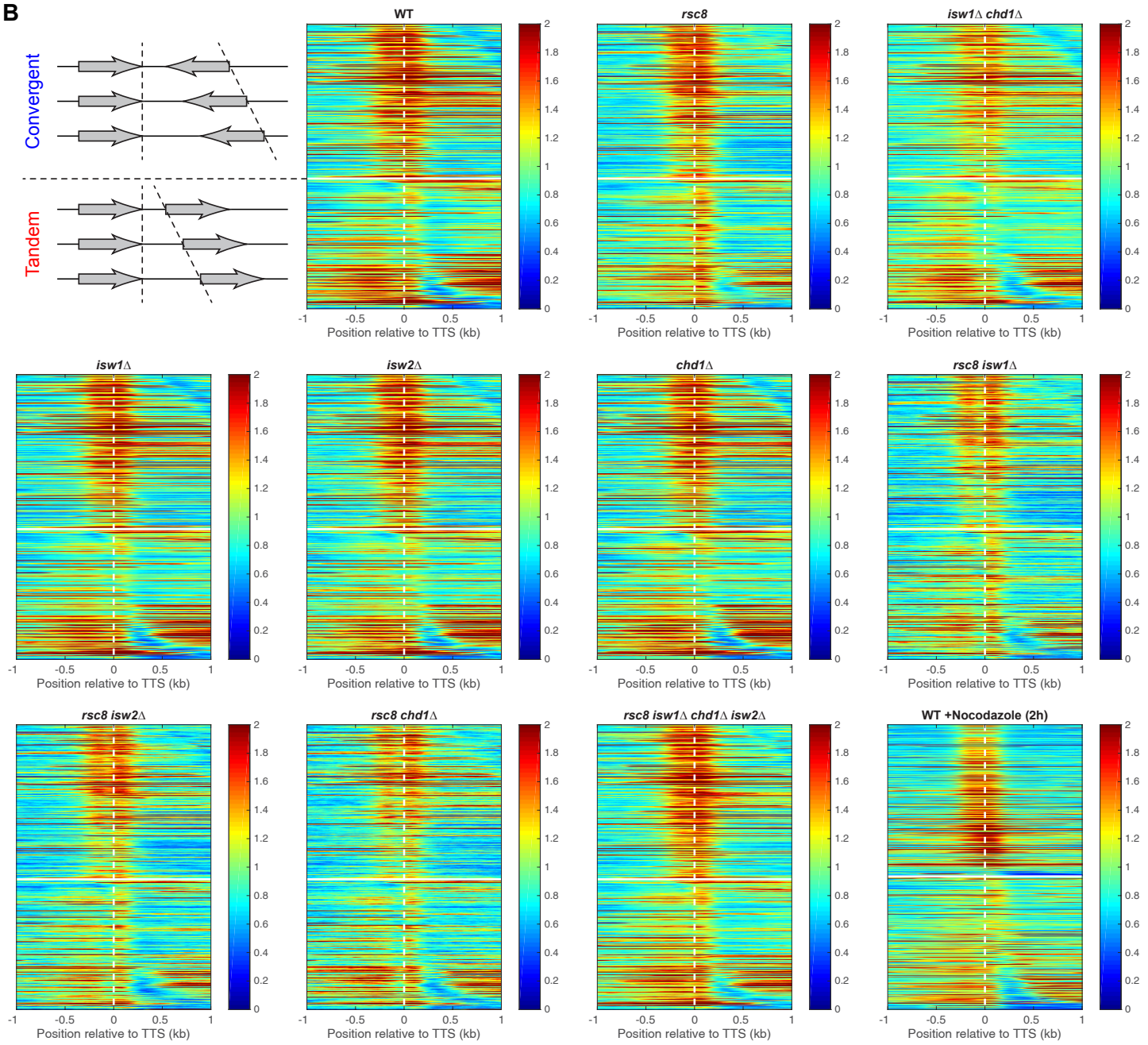

Supplemental Figure S6. (Continued.) (B) Heat maps for the data in A. Genes were aligned and sorted as in Fig. 3C. The white horizontal line separates convergent (top) from tandem gene pairs (bottom).

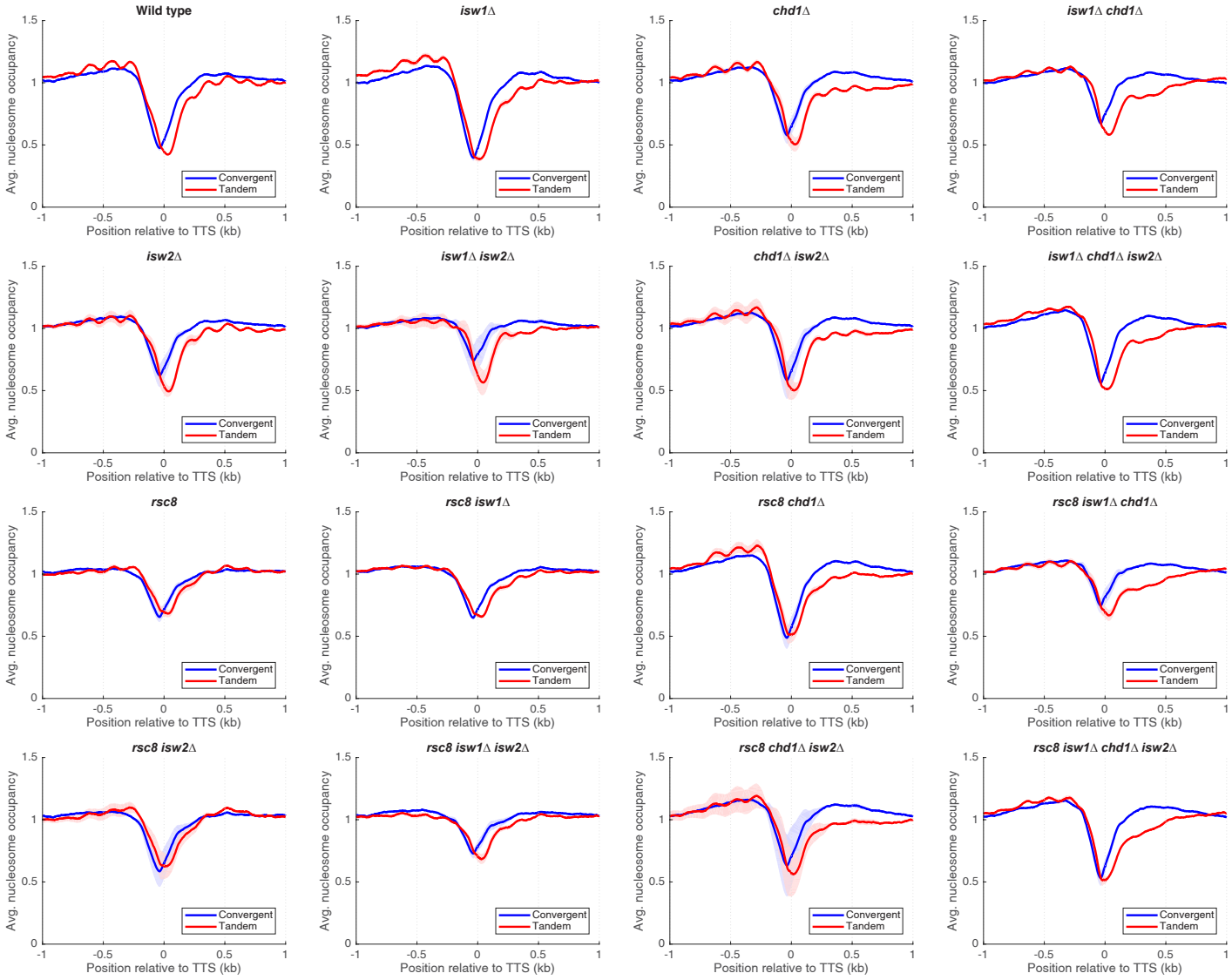

Supplemental Figure S7. Chromatin organization in the vicinity of the transcript termination site (TTS). Nucleosome occupancy aggregate plots for convergent and tandem gene pairs aligned on the TTS of the upstream gene. MNase-seq data normalized to the genomic average (set at 1). MNase-seq fragment sizes used: 120-180 bp.

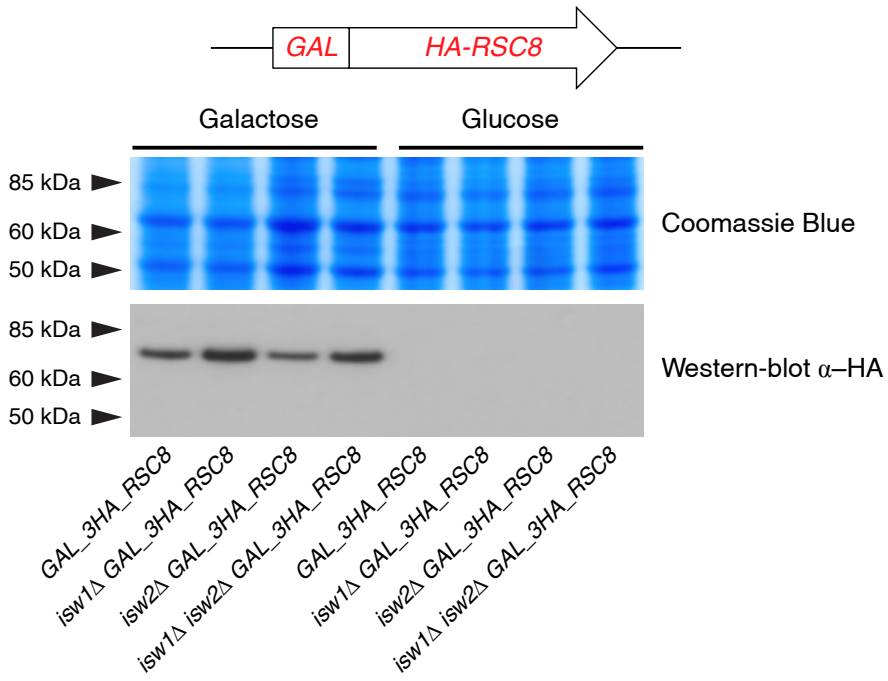

Supplemental Figure S8. Growth in glucose depletes *GAL-RSC8* strains of 3HA-tagged Rsc8. Western blot analysis of protein extracts from *GAL-RSC8* strains grown overnight in SC medium containing galactose and then switched to SC medium containing glucose for 7.5 hours at which point the cells stop growing. Upper panel: Coomassie blue staining of an SDS gel showing the total protein loaded. Lower panel: Detection of 3HA-tagged Rsc8 by Western blot using anti-HA-peroxidase antibody clone 3F10 (Roche 12013819001) and SuperSignal West Femto Maximum Sensitivity Substrate (Thermo Fisher Scientific 34095).

Supplemental Tables

Supplemental Table S1. Genotypes and sources of yeast strains used in this study. Strain construction is described in (Ocampo et al., 2016).

Strain	Genotype	Source
YTT186	*MATa ade2-1 can1-100 his3-11,15 leu2-3,112 trp1-1 ura3-1 RAD5+ isw1Δ::ADE2*	Tsukiyama et al. (1999)
YTT196	*MATα ade2-1 can1-100 his3-11,15 leu2-3,112 trp1-1 ura3-1 RAD5+ isw2Δ::LEU2*	Tsukiyama et al. (1999)
YJO504	*MATa/MATα ade2-1/ade2-1 can1-100/can1-100 his3-11,15/his3-11,15 leu2-3,112/leu2-3,112 trp1-1/trp1-1 ura3-1/ura3-1 RAD5+/RAD5+ ISW1/isw1Δ::ADE2 ISW2/isw2Δ::LEU2 rsc8::KanMX-GALp-HA3-RSC8*	Ocampo et al. (2016)
YJO505	*MATa/MATα ade2-1/ade2-1 can1-100/can1-100 his3-11,15/his3-11,15 leu2-3,112/leu2-3,112 trp1-1/trp1-1 ura3-1/ura3-1 RAD5+/RAD5+ ISW1/isw1Δ::ADE2 ISW2/isw2Δ::LEU2 RSC8/rsc8::KanMX-GALp-HA3-RSC8 CHD1/chd1Δ::HIS5*	Ocampo et al. (2016)
YPE458	*MATa ade2-1 can1-100 his3-11,15 leu2-3,112 trp1-1 ura3-1 RAD5+*	Ocampo et al. (2016)
YPE460	*MATa ade2-1 can1-100 his3-11,15 leu2-3,112 trp1-1ura3-1 RAD5+ isw1Δ::ADE2 isw2Δ::LEU2*	Ocampo et al. (2016)
YPE462	*MATa ade2-1 can1-100 his3-11,15 leu2-3,112 trp1-1ura3-1 RAD5+ isw1Δ::ADE2 rsc8::KanMX-GALp-HA3-RSC8*	This study
YPE464	*MATa ade2-1 can1-100 his3-11,15 leu2-3,112 trp1-1 ura3-1 RAD5+ isw2Δ::LEU2 rsc8::KanMX-GALp-HA3-RSC8*	This study
YPE466	*MATa ade2-1 can1-100 his3-11,15 leu2-3,112 trp1-1 ura3-1 RAD5+ isw1Δ::ADE2 isw2Δ::LEU2 rsc8::KanMX-GALp-HA3-RSC8*	This study
YPE468	*MATa ade2-1 can1-100 his3-11,15 leu2-3,112 trp1-1 ura3-1 RAD5+ rsc8::KanMX-GALp-HA3-RSC8*	This study
YPE470	*MATa ade2-1 can1-100 his3-11,15 leu2-3,112 trp1-1 ura3-1 RAD5+ isw2Δ::LEU2*	Ocampo et al. (2016)
YJO482	*MATa ade2-1 can1-100 his3-11,15 leu2-3,112 trp1-1 ura3-1 RAD5+ chd1Δ::HIS5*	Ocampo et al. (2016)
YJO484	*MATa ade2-1 can1-100 his3-11,15 leu2-3,112 trp1-1 ura3-1 RAD5+ isw1Δ::ADE2 chd1Δ::HIS5*	Ocampo et al. (2016)
YJO486	*MATa ade2-1 can1-100 his3-11,15 leu2-3,112 trp1-1 ura3-1 RAD5+ isw2Δ::LEU2 chd1Δ::HIS5*	Ocampo et al. (2016)
YJO488	*MATa ade2-1 can1-100 his3-11,15 leu2-3,112 trp1-1 ura3-1 RAD5+ isw1Δ::ADE2 isw2Δ::LEU2 chd1Δ::HIS5*	Ocampo et al. (2016)
YJO490	*MATa ade2-1 can1-100 his3-11,15 leu2-3,112 trp1-1 ura3-1 RAD5+ isw1Δ::ADE2 rsc8::KanMX-GALp-HA3-RSC8 chd1Δ::HIS5*	This study
YJO492	*MATα ade2-1 can1-100 his3-11,15 leu2-3,112 trp-1 ura3-1 RAD5+ isw2Δ::LEU2 rsc8::KanMX-GALp-HA3-RSC8 chd1Δ::HIS5*	This study
YJO493	*MATa ade2-1 can1-100 his3-11,15 leu2-3,112 trp1-1 ura3-1 RAD5+ isw1Δ::ADE2 isw2Δ::LEU2 rsc8::KanMX-GALp-HA3-RSC8 chd1Δ::HIS5*	This study
YJO494	*MATa ade2-1 can1-100 his3-11,15 leu2-3,112 trp1-1 ura3-1 RAD5+ rsc8::KanMX-GALp-HA3-RSC8 chd1Δ::HIS5*	This study
YDC111	*MATa ade2-1 can1-100 leu2-3,112 trp1-1 ura3-1*	Kim et al. (2006)

Supplemental References

Ganguli D, Chereji RV, Iben JR, Cole HA, and Clark DJ. 2014. RSC-dependent constructive and destructive interference between opposing arrays of phased nucleosomes in yeast. *Genome Res.* **24**: 1637–1649.

Kim Y, McLaughlin N, Lindstrom K, Tsukiyama T, and Clark DJ. 2006. Activation of *Saccharomyces cerevisiae* HIS3 results in Gcn4p-dependent, SWI/SNF-dependent mobilization of nucleosomes over the entire gene. *Mol Cell Biol* **26**: 8607–8622.

Ocampo J, Chereji RV, Eriksson PR, and Clark DJ. 2016. The ISW1 and CHD1 ATP-dependent chromatin remodelers compete to set nucleosome spacing in vivo. *Nucleic Acids Res.* **44**: 4625–4635.

Tsukiyama T, Palmer J, Landel CC, Shiloach J, and Wu C. 1999. Characterization of the imitation switch subfamily of atp-dependent chromatin-remodeling factors in saccharomyces cerevisiae. *Genes Dev.* **13**: 686–697.